Computational Electronics and Electromagnetics

Clifford C. Shang, Thrust Area Leader

January 1998

Computational Electronics and Electromagnetics

Clifford C. Shang,
Thrust Area Leader

January 1998

Clifford C. Shang, Thrust Area Leader

The Computational Electronics and Electromagnetics thrust area serves as the focal point for Engineering R&D activities for developing computer-based design and analysis tools. Representative applications include design of particle accelerator cells and beamline components; design of transmission line components; engineering analysis and design of high-power (optical and microwave) components; photonics and optoeletronics circuit design; electromagnetic susceptibility analysis; and antenna synthesis.

The FY-97 effort focuses on development and validation of 1) accelerator design codes; 2) 3-D massively parallel, time-dependent EM codes; 3) material models; 4) coupling and application of engineering tools for analysis and design of high-power components; and 5) development of beam control algorithms coupled to beam transport physics codes.

These efforts are in association with techology development in the power conversion, nondestructive evaluation, and microtechnology areas. The efforts complement technology development in Lawrence Livermore National programs.

Computational Electronics
and Electromagnetics

1. Computational Electronics and Electromagnetics

Overview
Clifford C. Shang, Thrust Area Leader

Technologies for Advanced Induction Accelerators

Maurice A. Hernandez
Defense Sciences Engineering Division
Electronics Engineering

In FY-97 we laid the groundwork for the development of a sophisticated system, capable of real-time control of the Heavy Ion Fusion (HIF) recirculating accelerator at Lawrence Livermore National Laboratory (LLNL). Our efforts included modeling the ion beam dynamics; designing and deploying a new injector pulser; and work to model, design, and test induction core modulators, as well as pulsers for the steering dipoles and insertion/extraction kickers.

Introduction

A 1991 study[1] showed that a recirculating ion beam accelerator (recirculator) is a promising candidate for a cost-effective driver for inertial fusion energy. Its promise is derived from the fact that the beam passes many times through each accelerating component; thus, fewer and more effective accelerating elements, as well as fewer focusing magnets, are required. This leads to a cost savings relative to a linear accelerator, which uses each accelerating core and focusing quadrupole only once per pulse (Fig. 1).

With the recirculator concept, we can also avoid beam resonance effects by using an active control system to rapidly ramp the bending field, and rapidly accelerate the beam (since the oscillating frequency of the particles in the confining field is rapidly changing, and hence is not resonant). Thus, much larger currents can be transported than are possible in a conventional synchrotron. However, these advantages are achieved at the expense of entering a regime in which the total path length traversed by the beam is greater, the repetition rate of the induction modules is higher, and the dynamics of transporting beams around the bends are unexplored.

These new and unexplored regimes make the development path leading to a small, scaled recirculator ground-breaking and rich in potential scientific discovery and technological innovation. The results of this project are expected to prove useful for a range of applications in defense and pure science.

As of the end of FY-97, several technology elements in this program are well along the development path to a complete recirculator. We have carried out a large complement of beam-transport modeling simulations, used to develop control algorithms and to help derive performance specifications on some accelerator components. A new injector pulser was developed that greatly enhanced the initial beam
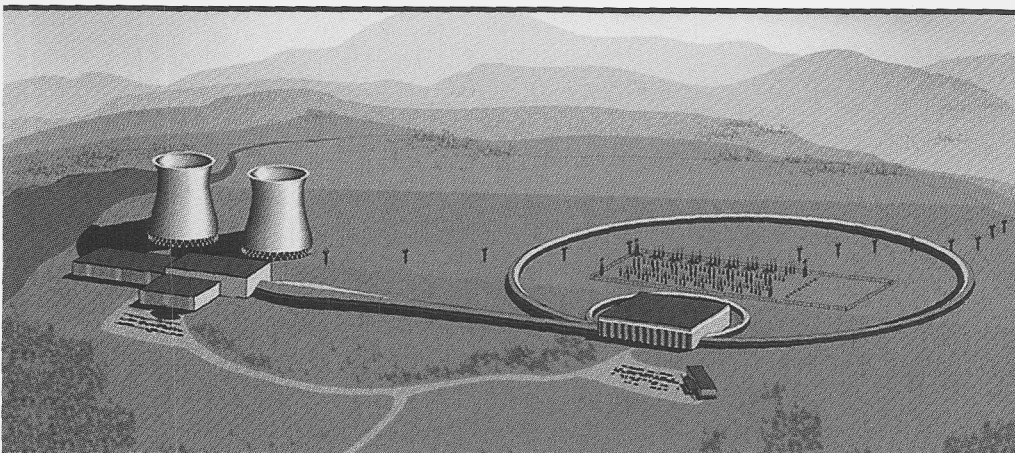
Figure 1. Conceptual drawing of a future Heavy Ion Fusion Power Plant.

quality. Matching and magnetic transport experiments have been carried out on a completed injector, matching section, and insertion section.

We have co-developed, with Lawrence Berkeley National Laboratory (LBNL), a pulser capable of dynamically driving the bending dipoles at the proper rate for beam steering. A similar pulser has been designed to drive the ion beam insertion/extraction kickers. The prototype induction modulator package has been built and tested extensively.

Significant further development, which will carry over into FY-98, will be necessary before the prototype can be replicated in quantity. We have completed construction of 10 half-lattice periods (modulator and dipole assemblies), enough to complete 90° of the recirculator. Tailored acceleration (adaptive control of modulator pulse characteristics) coupled with ramping of the dipole (bending) fields, to be addressed as part of our FY-98 work, is the next essential element for concept validation. We propose to build a full 360°-ring by some time around the end of FY-99. Our initial goal in the completed ring will be to transport the beam for fifteen laps.

Progress

Beam-Transport Modeling

We set out to answer a number of questions through the modeling of the beam-transport dynamics. The level of precision required for successfully transporting the beam around the recirculator factors into the specifications for many system components. Through modeling, we can determine the relative effects on beam quality of different errors in the injector, acceleration, steering, and sensor sub-systems. We can then focus our development efforts on those sub-systems that are most critical to successful beam transport. We were also able to evaluate the effectiveness of proposed control algorithms, and refine the algorithms to optimize the beam quality (**Fig. 2**).

Early modeling results pin-pointed the importance of initial (injected) beam quality, and identified the injector sub-system as a problem area. The voltage pulse produced by the original injector pulser created an ion beam with small, inherent errors. Subsequent beam acceleration magnified the errors, creating instabilities that make beam control more difficult. Because of these findings, an effort was initiated to redesign the injector pulser. The results are covered later in this report.

Our simulation strategy called for sensing the position of a pulse, then applying corrections to subsequent pulses as opposed to attempting to apply corrections to the same pulse on successive laps around the recirculator (a much more difficult implementation prospect). Matched centroid positions were calculated, with position and velocity corrections applied at succeeding bending dipoles. We then verified the corrections at subsequent sensors. Simulations were carried out assuming error-free sensors. In practice, we anticipate that sensor errors will be small compared to cumulative errors in the steering components.

Random errors were introduced in bend strength (simulating dipole pulser errors), bend and quadrupole alignment, and beam characteristics, (such as stability, oscillations, energy, and uniformity). Error magnitudes on the order of 1% to 2% were found to be sufficient to cause the beam to impact the accel-

Figure 2. Simulated beam centroid position, showing the results of applied steering. The dashed lines represent the accelerator tube wall. Beam diameter is approximately 2.5 cm.
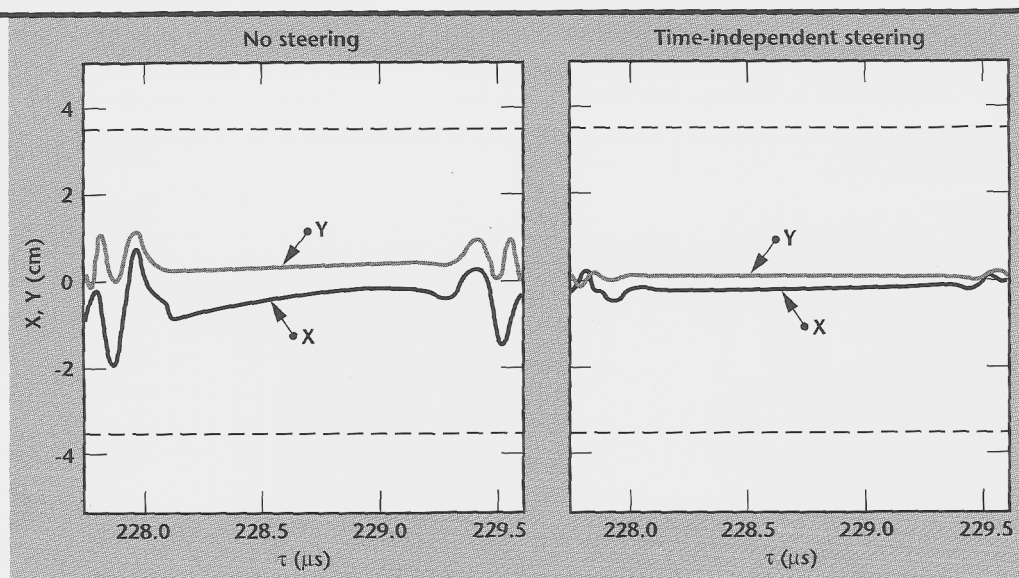
erator tube wall. Applying corrections as described in the previous paragraph demonstrated the ability to control the beam centroid within ±6 mm.

Design and Deployment of New Injector Pulser

As previously described, our modeling results revealed the need for redesigning our high potential ion source. The recirculator injector pulse modulators must be capable of producing very precise, repeatable voltage pulses to reduce the current modulation and achieve the required beam reproducibility. Initial beam control efforts will be focused on making corrections to the steering and acceleration waveforms on a pulse-to-pulse basis. Therefore, it is essential that the beam energy and timing from one pulse to the next are as nearly identical as possible. Modeling simulations have determined that errors greater than 0.1% in the flatness of the injector pulse can create intolerable beam energy deviations. Achieving these specifications pushes the limits of present pulse-power technology, including the methods used to measure the error in the modulator voltage pulse (**Fig. 3**).

To date, a new, higher voltage (120 kV), higher reliability pulse generator, which surpasses the previous generator in several key parameters, has been constructed, tested, and incorporated into the recirculator. The new generator produces a 5-μs pulse which is flat to less than ~0.1%. The rise and fall times of the pulse have an RC-type shape which is now adjustable by simply modifying resistor values. We have given a more detailed description of the new pulser in another report.[2]

During FY-98, we propose to conduct a complete assessment and characterization of the injector performance, including beam measurements.

Dipole and Kicker Pulser Development

The dipole and kicker pulsers make use of modeling and design efforts carried out at LBNL. As the recirculator ion beam is accelerated around the ring, it is gaining both kinetic and electrical energy. Thus, a larger electric field must be developed across each succeeding dipole pair to keep the beam centered in the beam tube. The pulser uses stacked transformers to achieve the required voltage levels and response.

Our recirculator design calls for driving the steering dipoles with a quadratic waveform ramping from 7 kV to 27 kV over a time span of 228 μs (the time required to complete 15 laps). Modeling results indicate that driving the dipoles with a fixed ramp will be sufficient to steer the beam within the required tolerances. This will require precise control of the induction core modulator (acceleration) waveforms. Part of our future work will involve investigating the option of varying the dipole driver waveform to adapt to acceleration errors. The present pulser design is adaptable to this option.

Induction Core Modulator Development

The recirculator requires state-of-the-art high-repetition rate and highly variable pulse modulators for the induction cores. Modulator specifications call for high bandwidth and dynamic power control, with the ability to produce a programmable wave with a high degree of flatness and reproducibility (<1% error) over the entire pulse length, and repetition rates on the order of 100 kHz (**Fig. 4**).

The initial modulator work has been conducted by researchers in LLNL's Power Conversion Technologies Thrust Area, resulting in a prototype which has been used for performance testing. The baseline modulator design contains two feedback paths: fast local feedback, with a single pole at 1.0 MHz, and a slower main feedback returned from the ferrite or Metglass cores. The ratio of feedback from these sources will be adjusted to maintain overall stability, while still maintaining a specified degree of waveform fidelity between the input and output signals. To date, one test-bed modulator has been constructed. Experimental results have
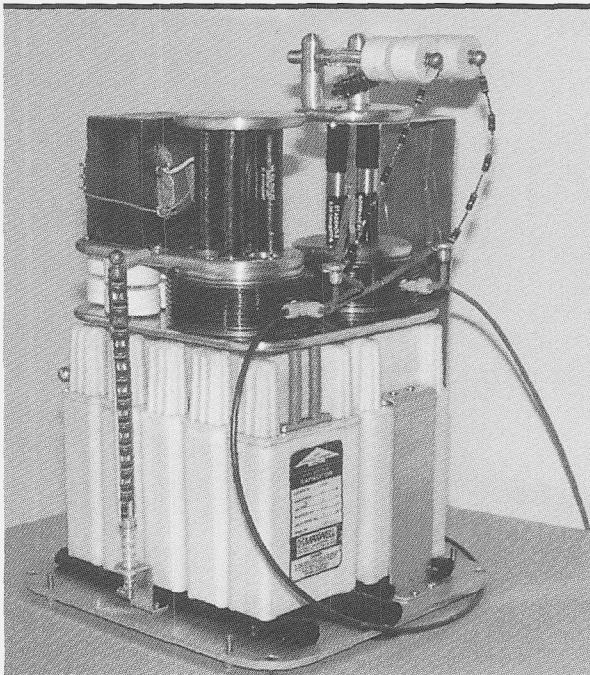

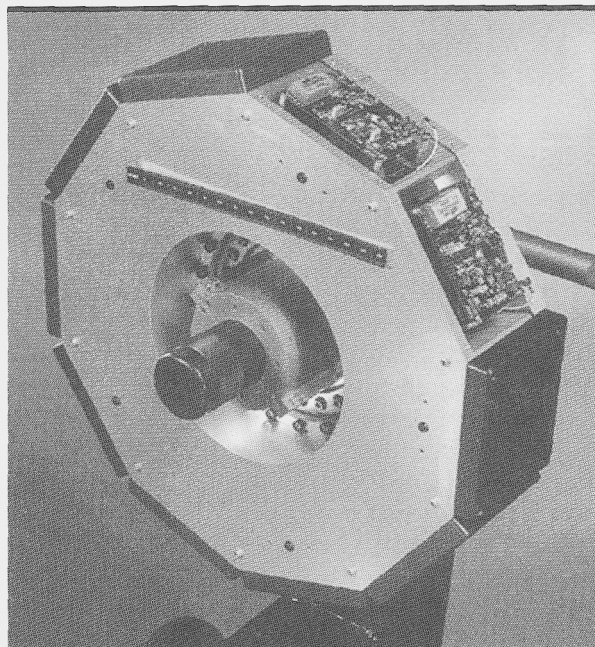Figure 3. Photograph of the new injector pulser.

Figure 4. Prototype induction modulator with the drive electronics covers removed.

demonstrated a very good correlation between the measured modulator output voltage and the modeling data. However, our modeling results have also shown that the level of overshoot exhibited by the prototype may be beyond the required error tolerance. We will address this issue as part of our future work.

Future Work

A large portion of the development and testing, as well as the integration of the modulators with the induction cores will be carried out as part of the proposed work for FY-98. Through funding provided by other sources, we will complete construction of 180° of the recirculator by October, 1998.

We also plan to incorporate the dipole pulser, modulator waveform shaping, and additional beam diagnostics into the recirculator. We will design and conduct experiments to study the beam-transport dynamics in the presence of these new components, and to verify our modeling results. This will include our initial attempts to apply shot-to-shot beam-control adjustments, the first step toward real-time control. These experiments will provide a better understanding of the control elements, and help us to refine our component and algorithm designs. We will also be able to assess the performance of our diagnostics in providing enough feedback to effectively control the beam.

Results of these experiments will be used to extend the technologies to the full recirculator (expected to be completed around October, 1999), and to other future accelerators which will require dynamic control. Further small-scale modeling efforts may be carried out to support the experimental work.

Acknowledgments

References

1. Barnard, J. J. (1991), *Study of Recirculating Induction Accelerators as Drivers for Heavy Ion Fusion*, Lawrence Livermore National Laboratory, Livermore, CA, (UCRL-LR-108095).

2. Wilson, M. J., D. A. Goerz, R. Speer, and R. Moal (1997), *Heavy Ion Fusion (HIF) Impulse Injector Design, Construction, and Checkout*, Lawrence Livermore National Laboratory, Livermore, CA, (in press).
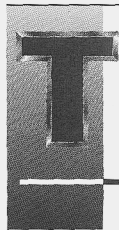
TIGER: An Object-Oriented Time-Domain Electromagnetics Simulation Code

David J. Steich, Jeffrey S. Kallman, and Gerald J. Burke
Defense Sciences Engineering Division
Electronics Engineering

This report discusses our progress to date and our future plans for the Time Domain Generalized Excitation and Response (TIGER) code. TIGER is an object-oriented computational electromagnetics (CEM) field solver. A prototype version of the TIGER code was completed this year. Preliminary results modeling a simplified 3-D kicker structure are shown. More than a 100-fold reduction in required cell count has been achieved, compared to previous modeling efforts. Our FY-98 plans include the parallelization of the TIGER code and the continued generalization and hybridization of the object-oriented framework.

Introduction

There is a significant need for more advanced time-domain CEM modeling capabilities related to the design of the Advanced Hydro Facility (AHF) at Lawrence Livermore National Laboratory (LLNL). Current CEM capabilities are represented by LLNL codes such as AMOS and TSAR, and by commercial codes such as MAFIA and XFDTD. These codes all have severe limitations, which include grid specific physics kernels; restricted material modeling capabilities; single-threaded physics methodologies; poor radiation boundary conditions; single-processor applicability (non MPP); simplified source inputs; and virtually non-existent interface algorithms. Many of these limitations occur because of historical scientific programming styles, largely induced by the use of FORTRAN, and preclude flexibility and extensibility. TIGER aspires to overcome these difficulties.

The development of a computational wakefield tool for the design of AHF accelerator components was the primary focus of our efforts this year. The design of a multi-pulse, multi-axis induction accelerator flash x-ray source for AHF requires development of accelerator components never designed before. Vital AHF components such as the induction cells, split beam-pipes, beam-line bends, and kicker structures require electromagnetic simulation to aid their design and ensure high beam-performance characteristics essential for the success of AHF.

The difficulty in accurately modeling these accelerator components can not be over-stated. Solving the full-wave physics of a high-space-charge-dominated electron beam being accelerated past induction cells, bent around corners, and split by kickers and septum magnets is presently an intractable problem using conventional 3-D particles-in-cell (PIC) codes. Even separating the problem into full-wave physics and beam-transport analysis regimes does not make the problem tractable. Beam-transport codes track beam dynamics such as beam envelope and centroid positions, but cannot be used where the beam experiences significant wakefields caused by perturbations in pipe cross-section. Currently, we are not directly addressing the beam-transport regime of modeling.

Our focus has been on the full-wave physics modeling required in areas where the pipe significantly changes cross-section, as is the case with the AHF components described above. These high wakefield regions can lead to beam instabilities known as beam break-up (BBU). To reduce the computational burden, linear electromagnetic full-wave physics calculations are performed to obtain wakefield impedances, under the assumptions that space charge effects can be ignored and that the wakefields do not influence the beam trajectory (that is, no coupling between wake fields and electron beam).

The first assumption is usually not of large concern, but must be kept in mind and checked whenever possible with analysis, experimentation, or with PIC simulations that include particle-particle interactions. To a large extent, the second assumption can be removed by post-processing the wakefield impedances and obtaining a better

approximation for the beam trajectory, then, in an iterative fashion, re-running the problem with the improved trajectory and obtaining improved wake-fields until convergence is achieved. These assumptions allow linear electromagnetic wakefield simulations to be used, which are much more efficient than PIC simulations. However, even linear electromagnetic wakefield calculations are intractable using present codes.

Progress

During the past year we successfully built a full working prototype version of TIGER, capable of modeling 3-D wakefield structures relevant to AHF. This prototype version implements our object-oriented memory and mesh management abstractions. Our goal was to test the usability, efficiency, flexibility, and extensibility of these abstractions in a real application setting. The physics kernel abstractions were implemented in elementary form. This allowed a much quicker working version of TIGER, and also provided a platform to test our on-going object-oriented research. The implementation of the wakefield physics and modeling of a simplified kicker structure (known as a Beam Position Monitor) was the primary emphasis of this year's thrust area project.

As a first example of TIGER's prototype capabilities, we considered the wake potential calculation of a relativistic electron beam going through a pillbox. We implemented a unstructured non-orthogonal discrete surface integral (DSI) method[1] to solve for the fields, using advanced radiation boundary conditions (RBCs),[2] and the latest in object-oriented techniques.[3,4]

Figure 1 shows a picture of the pillbox and a 2-D cross-section of the 3-D mesh blow-up of the pipe region. The pillbox height is 35 cm; the pipe radius is 1.1875 cm, and the gap width is 2 cm. A Gaussian pulse electron beam current source is used, with a full-width-half-maximum of 0.49486 ns. Quasi-analytic solutions exist for this problem.[5,6] The analytic solution of Weiland and Zotter assumes the pipe radius is zero.[5]

Shown in **Fig. 2** is a comparison of the two quasi-analytic solutions and TIGER. With this geometry, the solution of Weiland and Zotter overestimates the wake potential, especially near s = 0, due to the neglect of the finite pipe radius. The Dome solution takes into account the finite pipe radius, but neglects the frequency shifts in the solution due to the pipe. However, Dome states that this error is on the order of (pipe radius)^3/(gap length × pillbox radius)^2, which is ~ 0.000683.

The TIGER code used only 12,448 cells for this calculation. A TSAR calculation of this geometry using structured grid required just over a million cells. This example demonstrates TIGER's use of complex sources, advanced RBCs, general diagnostics, and wakefield formulations for a conforming, non-orthogonal, unstructured grid.
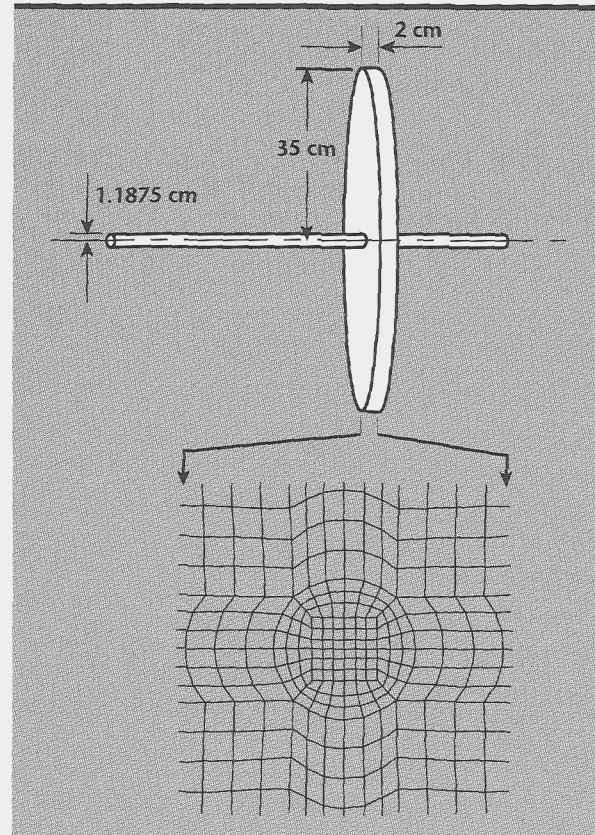

Figure 1. Two-dimensional mesh cross-section of three-dimensional pillbox.
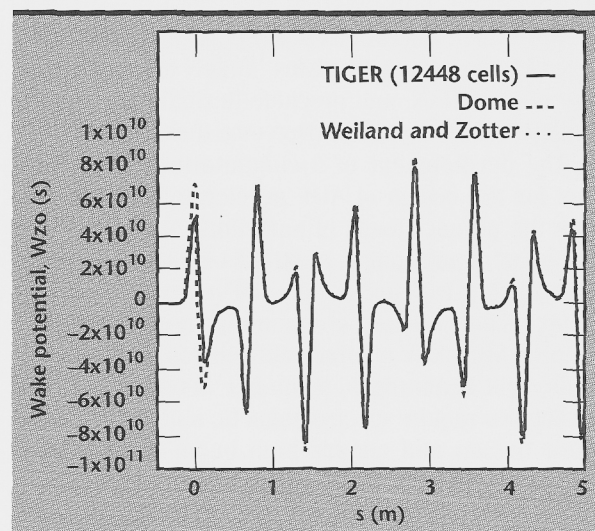

Figure 2. Wake potential comparison for pillbox geometry.

Next, we modeled a simplified kicker structure known a beam position monitor (BPM). Shown in **Fig. 3** is a picture of a BPM (the actual model did not include the beam-splitting section at the right in **Fig. 3**). For this example, each of the four kicker plates subtended 55° and was located at the unperturbed pipe radius. Modeling a BPM using TSAR required up to 30 million cells, 700+ MB RAM, weeks of CPU time, and was at the limit of what could be modeled. Thus, modeling a BPM would be a good demonstration of the new code.

We successfully modeled the BPM and compared results with existing simulation data and simplified analytic solutions. Over a 100-fold reduction in the number of cells was achieved with comparable or improved accuracy. This 100-fold reduction was accomplished by simultaneously using better boundary conditions (to truncate the problem space much closer to the kicker), conforming non-orthogonal grids (to avoid staircasing errors), extensive
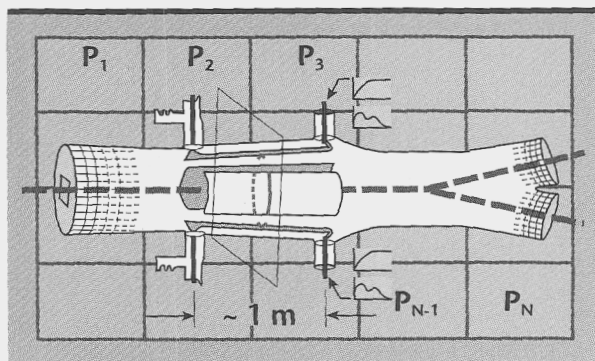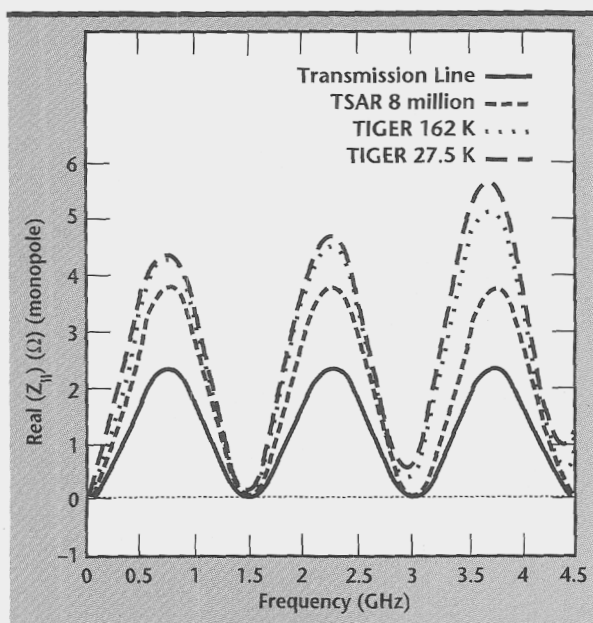

Figure 3. Kicker structure.

complex source modeling (to increase accuracy), and improved wakefield physics (to reduce both run time and required data storage).

Existing TSAR simulations required making two runs, gigabytes of data storage, at least a week of CPU time, and substantial post-processing. The new prototype code required only one run, kilobytes of data storage, two hours CPU time, and minimal post-processing. It also demonstrated new physics trends not shown in existing models.

Shown in **Figs. 4** and **5** are several preliminary TIGER results for the real and imaginary parts of the monopole wakefield impedance. The transmission line theory results are that of Ng[7] and do not take into account the cavity. The two TIGER results using 27.5K cells and 162.5K cells are in close agreement with one another, while the 8-million-cell TSAR result is further off. TSAR has only cubical cell capabilities, and so a staircased approximation was used for the BPM geometry. Due to the size of the model, running a more refined TSAR mesh was not possible using present resources.

Also shown in **Fig. 5** are 2-D results and an analytical solution of Heitfets and Kheitfets.[8] The designations, 'Heitfets and Kheitfets,' and '2-D no kicker,' correspond to results in the absence of the four kicker plates. Note the increasing trend of the analytic solution, the 2-D results, and the TIGER results. This increasing trend in imaginary longitudinal monopole impedance is due to the cavity. The transmission line theory does not take this into account. Note that the TSAR results also did not pick up the cavity part of the solution. It is unclear
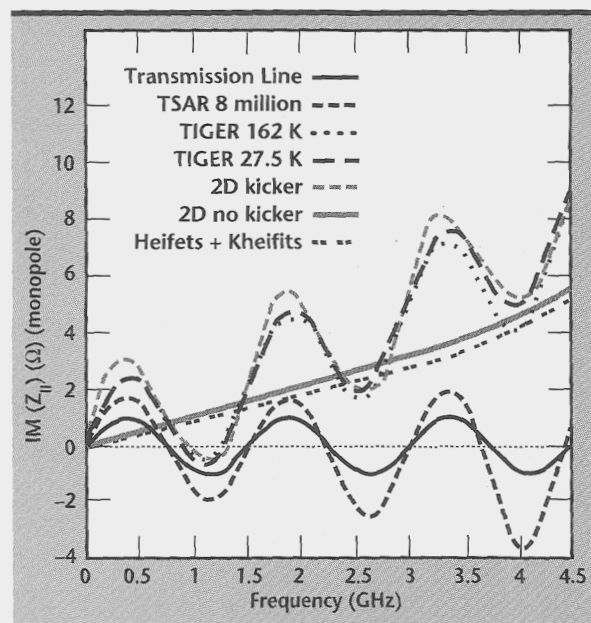

Figure 4. Real $Z_{\parallel}$ monopole results.

Figure 5. Imaginary $Z_{\parallel}$ monopole results.

at this time why TSAR is not picking up this bias trend in the results. It is also possible, although unlikely, that the TIGER results shouldn't show this upward trend in impedance. There is mounting evidence to suggest that the TIGER results are correct, but further research of these preliminary results still needs to be done.

Shown in **Figs. 6** and **7** is a similar set of results for the real and imaginary parts of the dipole transverse wakefield impedance of the BPM. Notice again, in **Fig. 7**, the amplitude shift for the imaginary part of the dipole impedance not being captured in the TSAR results. This constant displacement corresponds, through a frequency domain version of the Panofsky-Wenzel Theorem,

$$Z_\perp(\omega, r) = \frac{V}{\omega r_0} \nabla_\perp Z_\ell(\omega, r),$$

to a constant slope trend in the longitudinal impedance for m = 1, similar to that seen for m = 0, where m is the impedance mode number.

To test TIGER further, we did a series of test and validation exercises. Shown in **Fig. 8** are grid refinement tests indicating quick convergence of the TIGER results. **Figure 9** shows that the boundary conditions are very accurate for this test case and are not influencing the results with spurious reflections at the problem space truncation boundaries. **Figure 10** shows the calculated effective resistance modeling a 25-Ω coaxial feed using a 6-cell lumped

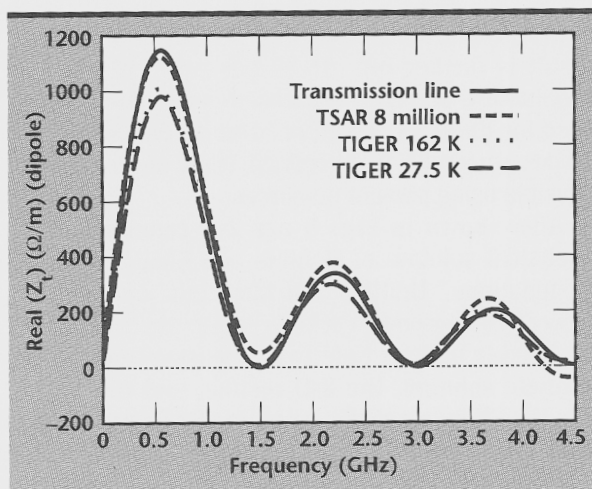Figure 6. Real Z_t dipole results.
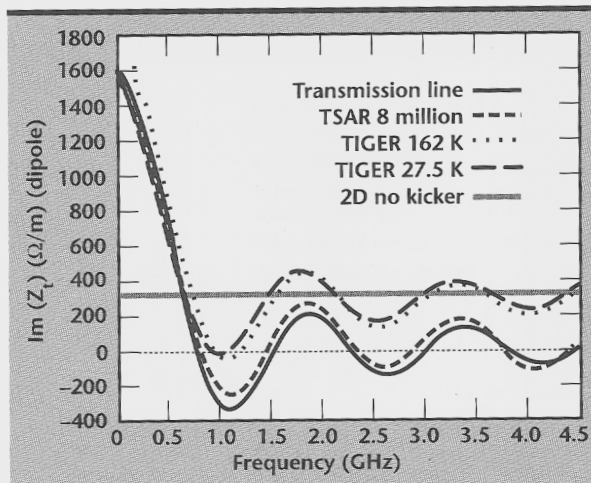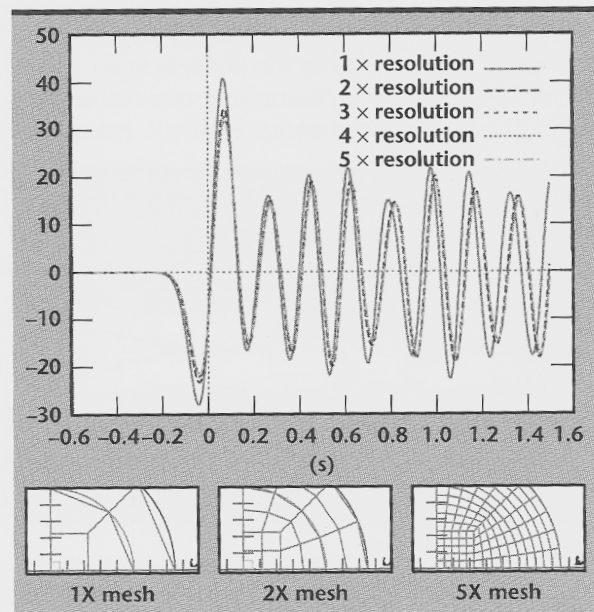

Figure 7. Imaginary Z_t dipole results.

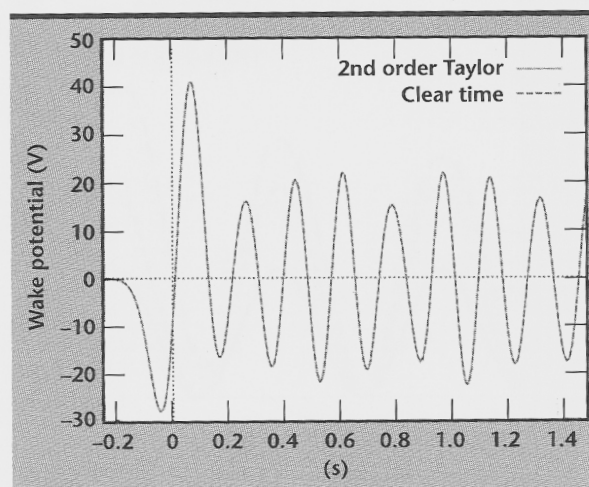Figure 8. Results of grid refinement tests.

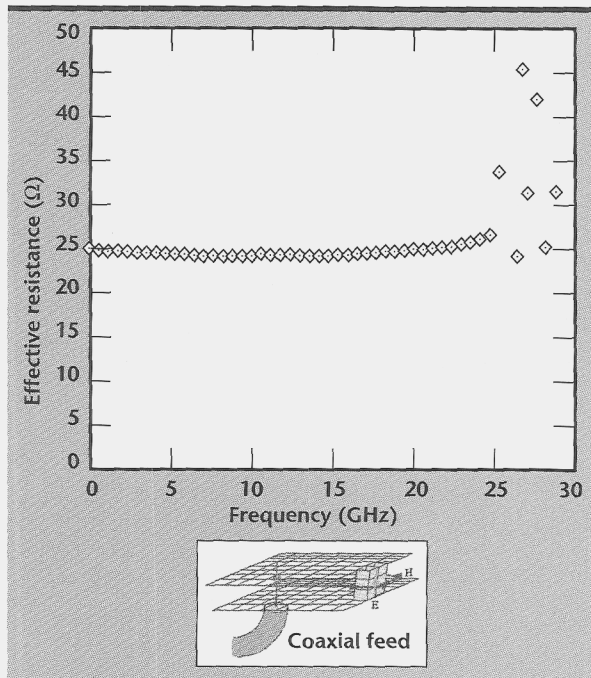Figure 9. Results of boundary condition convergence tests.

Figure 10. Results of coaxial feed modeling tests.

load resistor. The results show excellent agreement with the theoretical value of 25 Ω up to a frequency of 20 GHz, which is far above the highest frequency of interest.

Future Work

Next year, our focus will be on the enhancement of TIGER to include antenna and radar cross-section (RCS) sourcing and sensing capabilities. Specifically, we will be incorporating a near-to-far zone transform, antenna excitation capabilities, and antenna diagnostic capabilities. This will allow TIGER to excite antennas, compute radiation patterns, and provide output information such as input impedances, currents, and voltages for narrow- and wide-band situations.

Also, we will be looking into using PMESH, (a parallel platform meshing project) to help with our meshing concerns as we model more complex geometries.

Acknowledgment

References

1. Madsen, N. K., and R. W. Ziolkowski (1988), "Numerical Solution of Maxwell's Equations in the Time Domain Using Irregular Nonorthogonal Grids," *Wave Motion,* Vol. **10**, pp. 583–596.

2. Steich, D. J. (1995), Local Outer Radiating Boundary Conditions for the Finite-Difference Time-Domain Method Applied to Maxwell's Equations, Ph.D. thesis, Pennsylvania State University, Middletown, PA.

3. Veldhuizen, T. (1995), "Expression Templates," *C++ Report Magazine,* Vol. **7**, (5).

4. Myers, N. (1995), "A New and Useful Template Technique: 'Traits'," *C++ Report Magazine,* Vol. **7**, (5).

5. Weiland, T., and B. Zotter (1981), "Wake Potentials of a Relativistic Current in a Cavity," *Particle Accelerators,* Vol. **11**, pp. 143–151.

6. Dome, G. (1985), "Wake Potentials of a Relativistic Point Charge Crossing a Beam-Pipe Gap: An Analytical Solution," *IEEE Trans. Nuclear Science,* Vol. **NS-32**, pp. 2531–2534.

7. Ng, K.-Y. (1988), "Impedances of Stripline Beam-Position Monitors," *Particle Accelerators,* Vol. **23**, p. 93.

8. Heifets, S. A., and S. A. Kheifets (1991), "Coupling Impedance in Modern Accelerators," *Reviews of Modern Physics,* Vol. **63**, (3).

Multi-Scale Electrodynamics (MELD): A CAD Tool for Photonics Analysis and Design

Richard P. Ratowsky and Jeffrey S. Kallman
Defense Sciences Engineering Division
Electronics Engineering

Robert J. Deri and Michael D. Pocha
Electronics Engineering Technologies Division
Electronics Engineering

In FY-97 we completed work on the multi-scale electrodynamics (MELD) code, a comprehensive, multiple-length-scale, graphical user interface (GUI)-driven photonics design tool. In 1997, MELD was rated one of the one hundred most technologically significant new products of the year by *Research and Development* magazine.

Introduction

Photonics circuits using integrated and micro-optic devices are important because they will form the basis of all future high-speed and high-bandwidth communication systems, computers, and signal and image processing hardware. Computational simulation of these devices significantly reduces development and optimization time and cost. However, as photonics devices mature and increase in complexity, designers are faced with components that cannot be modeled using existing methods. A critical reason for this shortcoming is the presence of device feature sizes ranging from fractions of a wavelength to thousands of wavelengths, which are not amenable to a single numerical method.

As illustrated in **Fig. 1**, a photonics device or structure can be placed into one of three classes: optically large; optically small; or optically mixed, meaning large- and small-scale features are present in the same device.

Optically large components can be treated using beam propagation methods (BPM), which are, however, limited to unidirectional (paraxial) propagation. Optically small components can be modeled using codes that rigorously solve Maxwell's equations, such as finite-difference time-domain (FDTD) methods, to capture wavelength-scale physics. Optically mixed components are more difficult to model. If the length scales within the component can be decoupled to a good approximation, then hybrid methods using a combination of BPM methods

and Maxwell solvers in succession may be effective. However, for some problems, a decoupling of length scales is very difficult, or impossible.

To address these issues, the Photonics Analysis and Design project was proposed in FY-96 to create a comprehensive, multiple-length-scale, GUI-driven photonics design tool, which we call *MELD*, for multi-scale electrodynamics. MELD allows the user to compose a "virtual optical bench," where micro- or integrated-optical components can be laid out in a
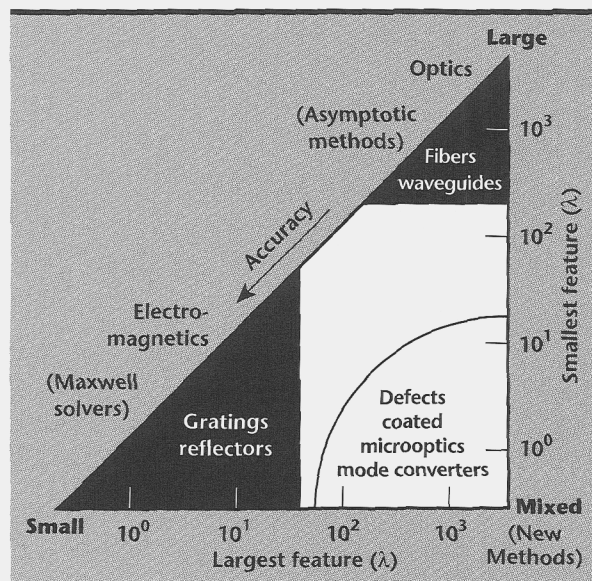

Figure 1. *Classification of photonics devices. In terms of largest and smallest feature size, photonics devices can be classified as optically large, optically small, or optically mixed.*

modular fashion. Each component is modeled using the most appropriate numerical method, and MELD provides a seamless interface between them.

Simulation in MELD begins when the user assembles an optical bench and "shoots light" from a source, such as a laser diode. Each module has one or more ports that can be connected to ports of other modules. MELD then propagates the light through the system, passing the transmitted field through the ports from one module to the next while keeping track of the reflected light. The optical field and intensities can be viewed at any port of the system. **Figure 2** shows the MELD 2-D layout for modeling an interferometer system.

Progress

In FY-97 we made a number of important advances in MELD to bring the project to its conclusion. These fall into three principal, but overlapping, areas: software, physics, and applications.

Software. We decided to rewrite the bulk of the underlying code using object oriented design in C++ ("new MELD"). Because of its modular structure,

each photonics module in MELD is naturally treated as an object, which allows a great deal of reusable code and greatly simplifies the introduction of new modules. Further, in FY-97 we generalized the virtual optical bench to allow 2-D layout, thus enabling modeling of important 2-D configurations, such as Michelson or Mach-Zender interferometers (**Fig. 2**). The previous version of MELD allowed only uniaxial propagation of light.

We also added optimization and scanning routines in FY-97. These allow MELD to perform automatically typical design calculations, such as maximizing coupling efficiency (light throughput) as a function of any system parameter; for example, transverse off-set of the source.

A final but essential software accomplishment was documentation. In anticipation of MELD's use outside of our group, we have created a basic user's manual for MELD[1] so the novice user can navigate the program.

Physics. The physics in MELD is embodied in the optical module algorithms. MELD now involves thirteen modules: aperture, free space, thin lens, spherical coated lens, coated dielectric plate,
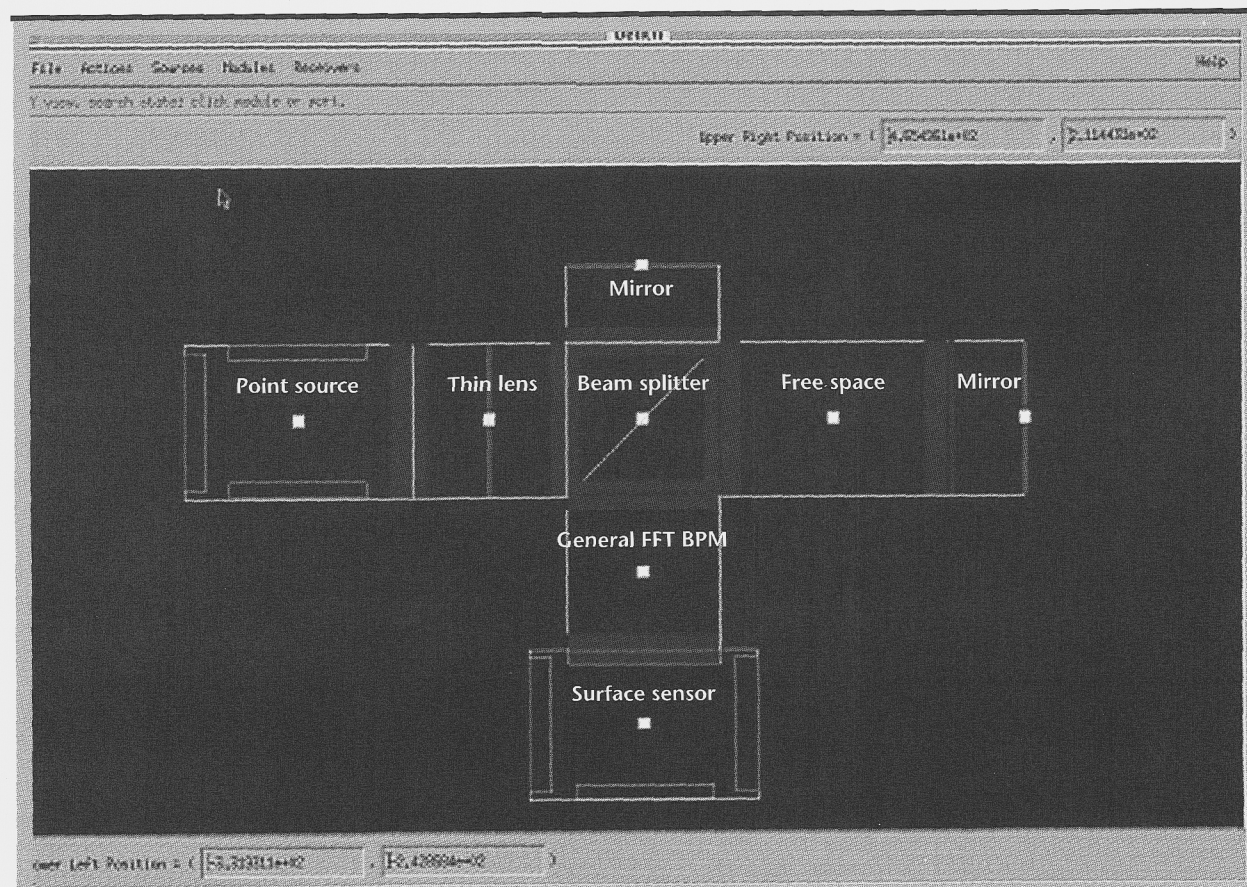

Figure 2. Two-dimensional layout of an interferometer in MELD.

directional coupler, mirror, phase plate, beam-splitter, ray-trace, general fast Fourier transform (FFT) BPM solver, FDTD Maxwell Solver, and transformer.

The BPM module solves the Helmholtz equation for optically large waveguiding structures. This module includes a full 3-D layout editor (written by us) for the system. The transformer is a "passive"

module that interpolates fields from one grid to another. Most of these modules were added in FY-97. The code framework for the FDTD and ray-trace modules were developed in FY-97, but they are not yet fully implemented in the new MELD.

The ray-trace algorithms under development in the MELD project deserve further explication, since
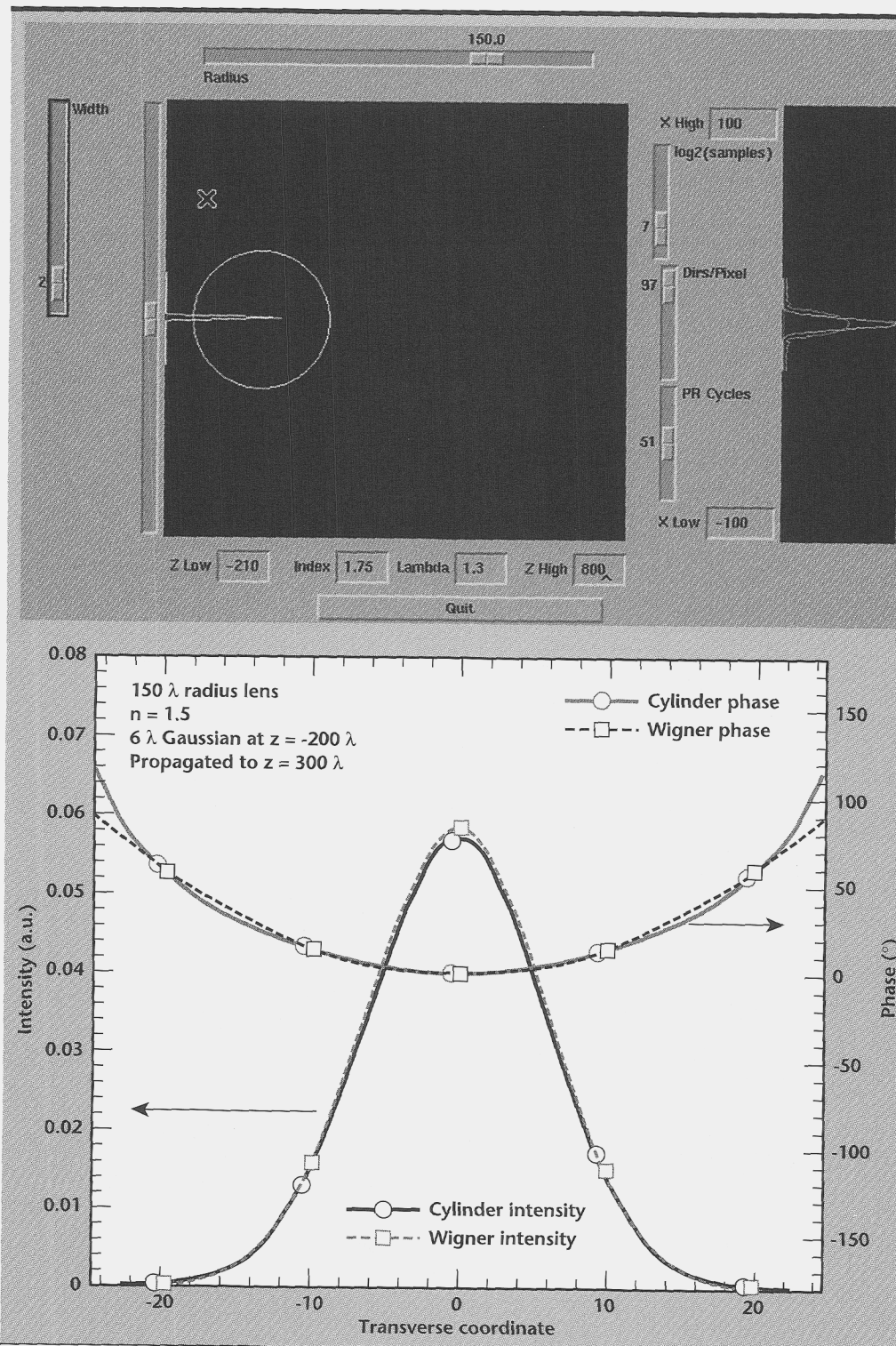

Figure 3. Accuracy of the Wigner method. A beam is propagated through a cylindrical lens very accurately. Curves marked "cylinder" are the exact solution. The user interface for the code is also shown.

they manifest the multi-scale spirit through the interface between ray and wave optics. Ray optics is usually a good approximation when the propagation medium is slowly varying on a wavelength scale. However, traditional ray optics cannot capture diffraction.

In FY-97 we developed and implemented an approach to ray optical propagation that allows us to calculate intensity and phase and, within a certain level of approximation, diffraction effects. The motivation for this work is the desire to model optically large elements, possibly with little symmetry, where diffraction effects may be important.

Our approach uses a set of rays distributed in both position and angle, called the Wigner distribution[2]. To propagate an optical beam, we first calculate the Wigner distribution from the complex field; it is equal to the Fourier transform of the two-point field correlation function of the field. We then simply propagate the Wigner distribution through the optical system from an input (source) plane to an output plane where we want to calculate the field. In practice, we propagate the rays backwards, since it is more convenient to know where a ray ends up than where it starts.

By projecting the output ray distribution in position (near field) and angle (far field), we can recover the phase of the field. This last step is accomplished using an iterative algorithm (Gerchberg-Saxon) which is identical to a technique used in the design of phase plates for LLNL's National Ignition Facility (NIF)[3]. Remarkably, then, we obtain both amplitude and phase information from the field from ray-tracing alone.

We illustrate the accuracy of the method in **Fig. 3**. Here we show the intensity and phase of a beam that has been propagated through a cylindrical lens using the Wigner method, compared with an "exact" calculation using an expansion in Bessel functions. The agreement is excellent, indicating that the method is potentially very valuable for treating aspherical surfaces, which are very difficult to model in any other way. This method is not yet implemented in a MELD module, but will be added in FY-98. It is now implemented in a stand-alone GUI-driven program (see **Fig. 3**).

Applications. We have had an ongoing relationship with Hewlett-Packard (HP) Laboratories, who continue to use MELD in the design of mode converters, components used to transform the optical mode size in a single-mode device to match that of a dissimilar device, thus increasing the coupling and relieving alignment tolerances. Optimal design of mode converters is an important issue, since a major limitation to the widespread use of photonic systems is the high cost (both in an economic and a performance sense) associated with this coupling.

HP has used MELD successfully to design a new mode-converter product line using ball lenses, an example of which is shown in **Fig. 4**, along with the MELD layout of the device package.

We have also created a World Wide Web interface to SPHERE, a subset (stand-alone module) of MELD which can be used for the mode-converter design. In FY-97 we also developed the capability to model arbitrary input fields, and this was used by HP to incorporate a realistic model of a novel laser diode design.

We have emphasized the uniqueness of MELD in being able to calculate, very accurately, coupling efficiencies for ball lens mode converters where other commercial software could not,[4–6] and to integrate different length-scale algorithms in a single package. Our results have been recognized through a 1997 award sponsored by *Research and Development* magazine as one of the one hundred most technologically significant new products of the year.[7]

Figure 4. The HP-designed mode-converter package (a), designed using MELD. The package includes a laser diode and 750-μm-diameter ball lens on a silicon submount; (b) shows the MELD GUI-layout of the device.
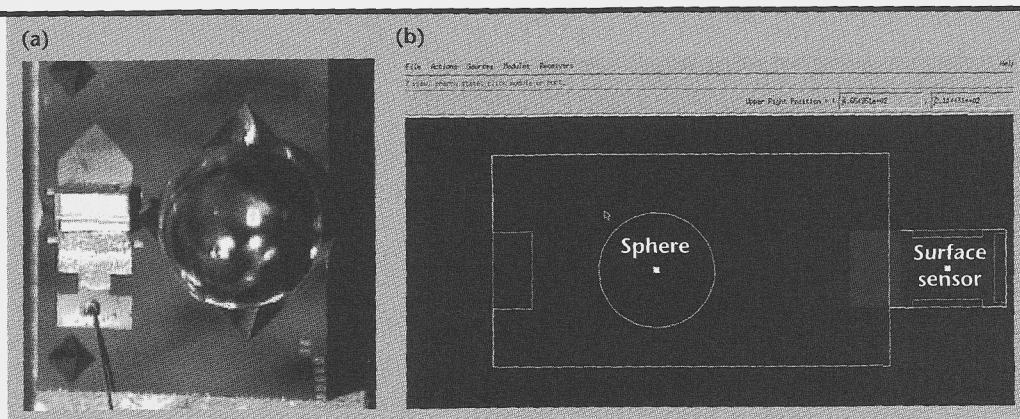
Future Work

While the two-year effort is now complete, MELD is certainly not a closed-end project, for two reasons. First, the existing code can always be improved: some capabilities we would like to see are not yet implemented to our satisfaction, such as the FDTD solver and the ray-trace module. Second, new modules can and should be added to MELD. Their selection will be driven by applications. Furthermore, to be widely accessible, the code should be ported to other platforms. MELD currently runs on UNIX workstations using MOTIF graphics. We are exploring options to commercialize the code and fund the additional improvements.

References

1. Kallman, J. S., and R. P. Ratowsky (1997), *Introduction to Multiscale ELectroDynamics (MELD)*, in press.

2. Wolf, E. (1978), "Coherence and Radiometry," *J. Opt. Soc. Am.* **68**, pp. 6–17. and M. Bastiaans (1997), "Application of the Wigner distribution function in optics," *The Wigner Distribution: Theory and Applications to Signal Processing*, W. F. G. Mecklenbräuker, Ed., North-Holland.

3. Dixit, S. N., M. D. Feit, M. D. Perry, and H. T. Powell (1996), "Designing fully continuous phase screens for tailoring focal plane irradiance profiles," *Opt. Lett.,* **21**, pp. 1715–17.

4. Ratowsky, R. P., L. Yang, R. J. Deri, J. S. Kallman, and G. Trott (1997), "Laser diode to single-mode fiber ball lens coupling efficiency: full-wave calculation and measurements," *Applied Optics,* **2005**, pp. 3435–3438.

5. Ratowsky, R. P., L. Yang, R. J. Deri, J. S. Kallman, and G. Trott (1995), "Ball lens reflections by direct solution of Maxwell's equations," *Opt. Lett.,* **20**, p. 2048.

6. Yang, L., K. W. Chang, G. Trott, R. P. Ratowsky, R. J. Deri, and J. S. Kallman (1995), "Micro-size ball lenses for micro-optics: theory and experiment," *Photonics West, San Jose, CA,* SPIE Vol. **2687**, January.

7. 1997 R&D 100 Awards, *Research and Development,* September, Vol. **39**, (10), p. 41.